

Composition profiling in a binary polymer blend thin film using polarized neutron reflectivity

H. GRÜLL¹(*), A. SCHREYER^{1,2}, N. F. BERK¹, C. F. MAJKRZAK¹ and C. C. HAN¹

¹ *Material Science and Engineering Laboratory, National Institute of Standards and Technology (NIST) - Gaithersburg, MD 20899-8542, USA*

² *Institut für Experimentalphysik/Festkörperphysik, Ruhr-Universität Bochum D-44780 Bochum, Germany*

(received 10 August 1999; accepted in final form 26 January 2000)

PACS. 83.80.Es – Polymer blends.

PACS. 82.65.Dp – Thermodynamics of surfaces and interfaces.

PACS. 61.12.Ha – Neutron reflectometry.

Abstract. – The concentration profile in an ultra-thin film (film thickness $d = 435 \text{ \AA}$) of a high molecular mass poly(isoprene)/deuterated poly(butadiene) blend is measured in the bulk system's miscible region with a new polarized neutron reflectivity method. By using a buried ferromagnetic layer inside the wafer and a polarized neutron beam, it is possible to obtain the neutron specular reflection amplitude A including its phase angle φ . Conventional reflectivity measurements only determine the reflected intensity $I = A^2$ which does not contain information on the phase angle. Only the knowledge of the phase angle allows an unambiguous determination of the neutron scattering length density profile of the film. The scattering length density profile thus obtained reveals poly(isoprene) segregating symmetrically to the polymer/air and polymer/Si interfaces. The adsorption profile at both interfaces can be approximately described using an exponential- or tanh-function with a decay constant smaller than the bulk correlation length.

When a binary mixture is brought into contact with an interface (solid substrate or air), the component with the lower surface free energy will preferentially adsorb to minimize the free energy of the system. In the case of polymer thin films, this adsorption can be symmetric with the same component going to both interfaces or asymmetric where the two interfaces favour different components or show no preferential attraction at all [1–15]. The case of symmetric adsorption or wetting on non-identical confining interfaces (*e.g.*, silicon (Si) *vs.* air) is less common and was only observed in a few cases [13–15]. In semi-infinite polymer films (“thick” films), the decay of the adsorption profile from surface composition, ϕ_s , to the bulk composition, ϕ_b , is expected to follow a functional form f , generally expressed as $\phi(z) \sim \phi_s \cdot f(z/\xi_s)$ (ϕ , volume fraction) with ξ_s comparable to the correlation length of the density fluctuations ξ_b [16–18] in bulk. An initial theoretical treatment using a mean-field approach was performed by Schmidt and Binder [16] predicting an adsorption profile in semi-infinite systems which decays exponentially towards bulk composition with a decay length comparable to ξ_b . More recent computer simulations suggest a tanh-shaped adsorption profile [17]. For films of a thickness d much larger than $4\xi_b$ the two interfaces are expected to be decoupled and to behave comparably to semi-infinite systems. These systems were

(*) Present address: Ben-Gurion University of the Negev, Department of Chemical Engineering, P.O. Box 653, Beer-Sheva 84105, Israel; e-mail: hgruell@bgumail.bgu.ac.il

thoroughly investigated [1–8]. Less experimental and theoretical work was done with finite systems of a film thickness, d , such that the adsorption profiles at two interfaces (polymer/air and polymer/Si, or two hard walls) can interact, $d \leq 4\xi_b$ [13, 19, 20].

Many experiments were performed to study the functional form of the adsorption profile of binary polymer blends either at the mixture/wall or mixture/air interfaces. The experimental results are controversial in their findings as well as in their interpretation within the framework of recent theories. Real space methods (*e.g.*, secondary ion mass spectroscopy [4], nuclear-reaction analysis [5], forward recoil spectroscopy [21, 22]) used to investigate the depth z -profile in polymer films usually have less instrumental resolution normal to the film x, y -plane than reciprocal space scattering techniques such as neutron reflectivity (NR). NR allows depth profiling with a spatial resolution on the order of angstrom (\AA) but the standard model-dependent analysis of reflection data [3, 6] does not provide unique information about the depth z -profile because there is no simple relation between the real space profile and the reflection intensity. Here, a NR method is presented which allows depth profiling in thin films with high depth resolution but does not depend on ambiguous model-dependent fitting of the reflection data. The technique is applied to study the composition profile of a polymer blend film with a thickness in the range where the adsorption layers are expected to interact.

In this study a new approach is used to obtain the complex neutron specular reflection amplitude using a buried reference layer inside the Si substrate. An iron layer of 50 \AA thickness is first sputtered onto a single crystal silicon substrate disc (10 cm diameter, 5 mm thick) and is then capped with a sputtered, smooth ($\sigma \sim 6 \text{\AA}$; σ , root-mean-square roughness) Si layer of about 100 \AA thickness. This wafer is used as a substrate to deposit an ultra-thin polymer blend film (d , film thickness; $d \approx 435 \text{\AA}$) of high molecular mass deuterated poly(butadiene) (dPB; $M_w = 104 \text{ kg/mol}$; $M_w/M_n = 1.06$) and poly(isoprene) (PI; $M_w = 142 \text{ kg/mol}$; $M_w/M_n = 1.03$ [23]) with an average composition of $\phi_{\text{PI}}^{\text{av},0} = 0.53$ (ϕ , volume fraction PI) by spin-coating from a toluene solution. A schematic depiction of the substrate is shown in the inset in fig. 1. The polymer blend dPB/PI shows lower-critical-solution-type phase behavior (LCST) and its bulk phase diagram has been characterized by SANS measurements. The interaction parameter χ shows a temperature dependence, $\chi(T) = 0.00541 - 1.4234/T$, with a critical temperature of $T_c = 54.5 \text{ }^\circ\text{C}$ and a critical composition $\phi_{\text{cr,dPB}} = 0.552$ (ϕ_{dPB} , volume fraction dPB) [24].

The buried iron reference layer can be magnetized (20 mT = 200 Gauss) and shows different scattering length densities (SLD) for neutrons polarized in the spin-up and spin-down states providing contrast variation. Two polarized beam NR experiments with spin-up and -down neutrons, respectively, were performed at $T = 25 \text{ }^\circ\text{C}$ in the bulk system's miscible single-phase region. An algebraic reduction of these two measurements gives two possible reflection amplitudes, one of which is physically meaningless. The physically meaningful branch of the complex reflection amplitude $A = R \cdot \exp[i\varphi]$ can be fitted simultaneously and unambiguously to yield the SLD profile of the film. It is important to note that conventional reflectivity measurements only determine the reflected intensity $I = A^2 = R^2$, *i.e.* the information on the phase angle φ is not accessible in the experiment. Therefore, a fit of a composition profile to a measured intensity is in principle never unique. The novelty of the method used here is the contrast variation via the use of polarised neutrons and the iron reference layer in a reflectivity experiment which allows to extract the reflection amplitude A including the phase angle φ in the region of dynamical scattering. A fit to A then is in principle unique within the limits of statistics and the finite scattering vector range of the data. The SLD profile is described by parametric B-splines, *i.e.* independent of any models containing thickness or functional forms of interfaces [25]. A detailed description of this method with its first application to a metallic model system [26] and the explicit data reduction of this experiment

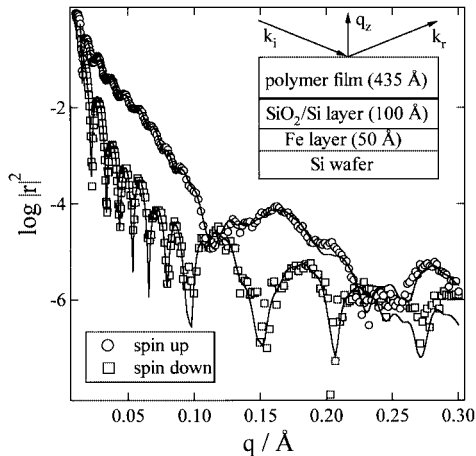


Fig. 1

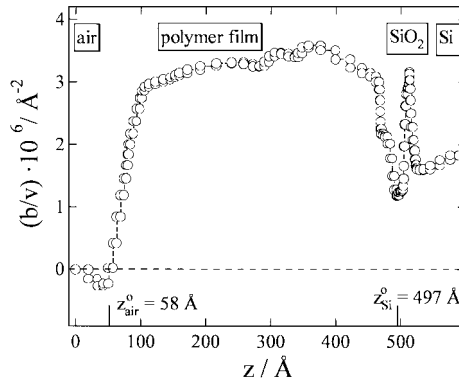


Fig. 2

Fig. 1 – Polarized neutron reflectivities as a function of q (q , scattering vector; $q = 4\pi/\lambda \cdot \sin\theta$; λ , neutron wave length with $\lambda = 4.76 \text{ \AA}$; θ , scattering angle) taken with spin-up and spin-down polarized neutron beams. At lower q ($q \leq 0.2 \text{ \AA}^{-1}$) the standard deviation is smaller than the symbol size, at higher q it corresponds to half a decade on the log scale. The small inset shows a schematic drawing of the sample structure consisting of the polymer film on top of a wafer with a buried iron reference layer.

Fig. 2 – The scattering length density (SLD) profile obtained by using the phase fitting method [27]. The air/polymer interface z_0 is defined where the SLD data become positive as both polymers have positive (b/v) values ((b/v) , scattering length density; $(b/v)_{\text{dPB}} = 6.64 \cdot 10^{-6} \text{ \AA}^{-2}$; $(b/v)_{\text{PI}} = 0.26 \cdot 10^{-6} \text{ \AA}^{-2}$).

are provided elsewhere [27]. Similar neutron reflection experiments requiring three contrast variation measurements have been discussed earlier [28–32].

Figure 1 shows the reflectivity curves taken with a polarized neutron beam in the spin-up and spin-down state while the reference iron layer is magnetized. The obtained SLD profile is plotted in fig. 2. The SLD profile has some degree of uncertainty because of statistical error in the raw data and the limitation of a truncated data set. It is difficult, however, to characterize this functional uncertainty, say with error bars on the SLD, since q -space uncertainties are distributed in z -space, and similar looking profiles can produce very different reflection amplitudes over a given q -range. Thus for now it is necessary to rely on physical judgement in assessing the model-independent SLD resulting from the analysis. For example, the deviation towards small negative SLDs can be deemed physically unrealistic because both polymers have a positive SLD ($(b/v)_{\text{dPB}} = 6.64 \cdot 10^{-6} \text{ \AA}^{-2}$; $(b/v)_{\text{PI}} = 0.26 \cdot 10^{-6} \text{ \AA}^{-2}$). Therefore, the z -value where the SLD profile becomes positive is taken as the polymer/air interface. Also, it seems unlikely for physical reasons that the SLD profile exhibits a small sinusoidal undulation in the middle of the polymer film and close to the Si-interface, although these observations should not *a priori* be discarded as meaningless. The SLD profile is converted to a composition profile using the relation $(b/v) = (b/v)_{\text{dPB}} \cdot \phi_{\text{dPB}} + (b/v)_{\text{PI}} \cdot \phi_{\text{PI}}$, ($\phi_{\text{PI}} + \phi_{\text{dPB}} = 1$), shown in fig. 3(a) and (b). The adsorption of PI at the polymer/air and polymer/Si surface is fairly symmetric reaching a surface composition of $\phi_{\text{s,air}} = 1$ at the air interface, whereas the surface composition at the polymer/Si interface is slightly lower $\phi_{\text{s,Si}} = 0.86$. The calculated average film composition using the composition profile shown in fig. 3(a) is $\phi_{\text{PI}}^{\text{av}} = 0.54$ which is close

TABLE I – Fitting parameters for the composition profile shown in fig. 3. The uncertainties ($\pm\sigma$) were evaluated by a standard statistical data analysis from linear regression of data. exp: $\phi = \phi_c + \Delta\phi \exp[-(\tilde{z}/\xi_s)]$; tanh: $\phi = \phi_c + \Delta\phi\{1 - \tanh(\tilde{z}/\xi_s)\}$ (with $\Delta\phi = \phi_s - \phi_c$; $\tilde{z}_{\text{air}} = z - z_{\text{air}}^0$; $\tilde{z}_{\text{Si}} = z_{\text{Si}}^0 - z$; $z_{\text{air}}^0 = 57.8 \text{ \AA}$; $z_{\text{Si}}^0 = 497 \text{ \AA}$).

Fixed center composition						
	ϕ_c	$\Delta\phi_{\text{air}}$	$\xi_{s,\text{air}}/\text{\AA}$	ϕ_c	$\Delta\phi_{\text{Si}}$	$\xi_{s,\text{Si}}/\text{\AA}$
exp	0.4964 (fixed)	0.5106 ± 0.013	34 ± 1.4	0.4964 (fixed)	0.370 ± 0.012	34 ± 1.4
tanh	0.4964 (fixed)	0.5998 ± 0.020	49 ± 2.0	0.4964 (fixed)	0.357 ± 0.011	36 ± 1.2
Best fit for each interface						
	$\phi_{c,\text{air}}$	$\Delta\phi_{\text{air}}$	$\xi_{s,\text{air}}/\text{\AA}$	$\phi_{c,\text{Si}}$	$\Delta\phi_{\text{Si}}$	$\xi_{s,\text{Si}}/\text{\AA}$
exp	0.5241 ± 0.006	0.4960 ± 0.013	29 ± 1.5	0.5026 ± 0.005	0.365 ± 0.013	25 ± 1.6
tanh	0.5352 ± 0.004	0.4813 ± 0.010	38 ± 1.4	0.5046 ± 0.005	0.350 ± 0.010	34 ± 1.7

to the expected value as a mixture of the composition $\phi_{\text{PI}}^{\text{av},0} = 0.53$ was deposit. Additional atomic force microscopy measurements at $T = 25^\circ\text{C}$ after film preparation prior to the NR experiment show a root-mean-square roughness of $\sigma = 6 \text{ \AA}$ for the polymer/air interface.

Various functional forms such as an error function, tanh [17], exponential [5, 16], double exponential and stretched exponential [3] were tested. None of these functions describes the adsorption profile perfectly. Introducing a stretched exponential or double exponential did not improve the fit as the fit parameters are strongly coupled, whereas an error functional profile could be completely discarded. The decay of the adsorption profile from each surface composition ϕ_s towards the film center composition ϕ_c can be well described using either a single exponential function $\phi = \phi_c + \Delta\phi \cdot \exp[-(\tilde{z}/\xi_s)]$ with a decay length ξ_s or a tanh function $\phi = \phi_c + \Delta\phi \cdot \{1 - \tanh(\tilde{z}/\xi_s)\}$ (with $\Delta\phi = (\phi_s - \phi_c)$; air-side: $\tilde{z} = z - z_{\text{air}}^0$; Si-side: $\tilde{z} = z_{\text{Si}}^0 - z$; z^0 , position of the interface). The fitting parameters are given in table I. Although the exponential and tanh function fits have slightly different shapes, these fits are of comparable

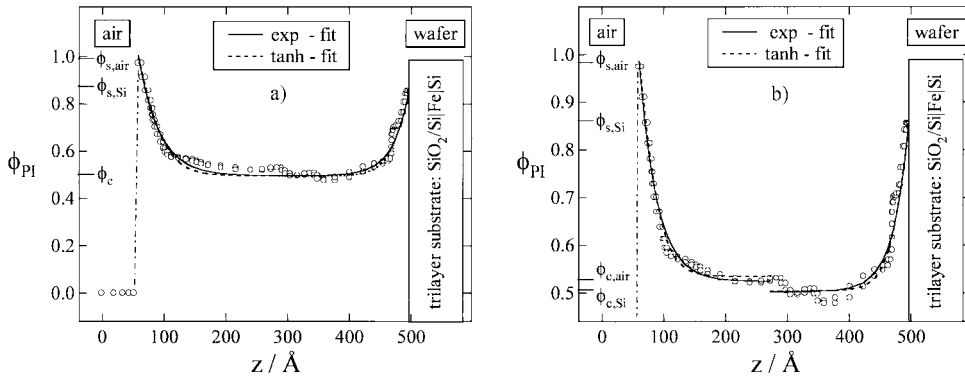


Fig. 3 – Calculated composition profiles in ϕ_{PI} (ϕ_{PI} , volume fraction poly(isoprene)) for the SLD profile using $(b/v) = (b/v)_{\text{dPB}} \cdot \phi_{\text{dPB}} + (b/v)_{\text{PI}} \cdot \phi_{\text{PI}}$. (a) Fits with a fixed center composition, (b) best fit of the interfacial regions for each half of the film. The fit parameters are given in table I.

quality if χ^2 is taken as a measure. For the fits shown in fig. 3(a), the center composition ϕ_c was kept constant and set to an average value of ϕ_c corresponding to the average composition in the film center in the range $220 < z/\text{Å} < 380$. This allows the two exponential fits of either interface to match in the center of the film. Allowing ϕ_c to vary as a fit parameter for each interface describes the air profile slightly better with a smaller decay length $\xi_{s,\text{air}}$, whereas the decay length $\xi_{s,\text{Si}}$ is almost unaffected. Not keeping ϕ_c constant leads to a slight mismatch in the film center due to the small sinusoidal composition variation shown in fig. 3(b), which was mentioned earlier. The value of ϕ_c is slightly lower than the average film composition due to the depletion of PI in the film center. It should again be emphasized that these are fits to data points describing the profile and not functional forms used in a model-dependent method to describe reflectivity data.

The decay lengths at both interfaces are of similar magnitude (exponential fits: $\xi_{s,\text{air}}^{\text{exp}} = 30 \text{ Å}$; $\xi_{s,\text{Si}}^{\text{exp}} = 26 \text{ Å}$; tanh fits: $\xi_{s,\text{air}}^{\text{tanh}} = 38 \text{ Å}$; $\xi_{s,\text{Si}}^{\text{tanh}} = 34 \text{ Å}$) and therefore are a factor of 3 to 4 smaller than the bulk phase correlation length, ξ_b , at $T = 25^\circ\text{C}$ ($\xi_b(T = 25^\circ\text{C}) \approx 110 \text{ Å}$ [24]). The film thickness, $d = 435 \text{ Å}$, is about 4 times larger than the bulk correlation length, $d \sim 4\xi_b$. Therefore, a coupling of surface interactions at both interfaces can lead to smaller surface correlation lengths ξ_s . Since the framework of the Schmidt-Binder theory suggesting an exponential profile is not expected to strictly hold under these conditions, a deviation is not surprising. Nevertheless, the adsorption profile in films of this thickness can be well approximated by an exponential form, although the data suggest a small deviation from simple exponential decay. Strong surface segregation as well as confined geometry effects may lead to changes in the phase behavior of polymer thin films such as a shift of the phase diagram. As no characterization of the phase behavior of this system under these conditions is available at this point of the study, any further interpretation in this direction is speculative. This model system dPB/PI shows the very unusual case of an almost symmetric segregation of PI to both interfaces although the confining surfaces air/polymer and polymer/Si are very different in nature. The much more common picture is that asymmetric confinement produces an asymmetric adsorption [1–8] or leads to a bilayer-type structure in case of coexisting phases [9, 11, 12]. As the interactions between the polymer and the substrate are extremely sensitive to sample preparation [15], fine tuning of these interactions can be used to control the internal morphology of a film [14] and switch from a bilayer to a trilayer structure. Here, the model-independent and unambiguous depth profile clearly shows that a stable trilayer-type structure is also possible in much thinner films.

In summary, a new NR method was used to obtain the depth profile in thin films of a binary polymer blend. This profile is unambiguous compared to a depth profile obtained using a model-dependent analysis in standard NR experiments. The adsorption of PI is found to be symmetric at both interfaces reaching surface compositions of $\phi_{s,\text{air}} = 1$ and at the Si interface $\phi_{s,\text{Si}} = 0.86$. The shape of the adsorption profiles can be approximated by either using a single exponential or hyperbolic tangent function although the data suggest a more complicated profile. The decay lengths at both interfaces have comparable magnitudes and are approximately 3 to 4 times smaller than the bulk correlation length ξ_b at the same temperature. In general, this method offers the possibilities to obtain depth profiles without the ambiguity of conventional NR data analysis. The method can be employed in future work to resolve key issues dealing with depth profiling problems in polymer physics.

* * *

HG and AS would like to thank the Alexander von Humboldt-Foundation for financial support. We gratefully thank H. JINNAI and T. HASHIMOTO for providing us with the sample.

REFERENCES

- [1] SOKOLOV J., RAFAILOVICH M. H., JONES R. A. L. and KRAMER E. J., *Appl. Phys. Lett.*, **54** (1989) 590.
- [2] JONES R. A. L., KRAMER E. J., RAFAILOVICH M. H., SOKOLOV J. and SCHWARZ S. A., *Phys. Rev. Lett.*, **62** (1989) 280.
- [3] JONES R. A. L., NORTON L. J., KRAMER E. J., COMPOSTO R. J., STEIN R. S., RUSSELL T. P., MANSOUR A., KARIM A., FELCHER G. P., RAFAILOVICH M. H., SOKOLOV J., ZHAO X. and SCHWARZ S. A., *Europhys. Lett.*, **12** (1990) 41.
- [4] ZHAO X., ZHAO W., SOKOLOV J., RAFAILOVICH M. H., SCHWARZ S. A., WILKENS B. J., JONES R. A. L. and KRAMER E. J., *Macromolecules*, **24** (1991) 5991.
- [5] ZINK F., KERLE T. and KLEIN J., *Macromolecules*, **31** (1998) 417.
- [6] NORTON L. J., KRAMER E. J., BATES F. S., GEHLEN M. D., JONES R. A. L., KARIM A., FELCHER G. P. and KLEB R., *Macromolecules*, **28** (1995) 8621.
- [7] SCHEFFOLD F., BUDKOWSKI A., STEINER U., EISER E., KLEIN J. and FETTERS L. J., *J. Chem. Phys.*, **104** (1996) 8795.
- [8] BUDKOWSKI A., SCHEFFOLD F., KLEIN J. and FETTERS L. J., *J. Chem. Phys.*, **106** (1997) 719.
- [9] SCHEFFOLD F., EISER E., BUDKOWSKI A., STEINER U., KLEIN J. and FETTERS L. J., *J. Chem. Phys.*, **104** (1996) 8786.
- [10] STEINER U., KLEIN J. and FETTERS L. J., *Phys. Rev. Lett.*, **72** (1994) 1498.
- [11] KERLE T., KLEIN J. and BINDER K., *Phys. Rev. Lett.*, **77** (1996) 1318.
- [12] KERLE T., KLEIN J. and BINDER K., *Eur. Phys. J. B*, **7** (1999) 401.
- [13] KARIM A., SLAWECKI T. M., KUMAR S. K., DOUGLAS J. F., SATIJA S. K., HAN C. C., RUSSELL T. P., LIU Y., OVERNEY R., SOKOLOV O. and RAFAILOVICH M. H., *Macromolecules*, **31** (1998) 857.
- [14] GENZER J. and KRAMER E. J., *Phys. Rev. Lett.*, **78** (1997) 4946.
- [15] KRAUSCH G., DAI C. A., KRAMER E. J., MARKO J. F. and BATES F. S., *Macromolecules*, **26** (1993) 5566.
- [16] SCHMIDT I. and BINDER K., *J. Phys.*, **46** (1985) 1631.
- [17] HARIHARAN A., KUMAR S. K. and RUSSELL T. P., *Macromolecules*, **24** (1991) 4909.
- [18] BRAZHNİK P. K., FREED K. F. and TANG H., *J. Chem. Phys.*, **101**(1994) 9143.
- [19] HARIHARAN A., KUMAR S. K., RAFAILOVICH M. H., SOKOLOV J., ZHENG X., DUONG D. H., SCHWARZ S. A. and RUSSELL T. P., *J. Chem. Phys.*, **99** (1993) 656.
- [20] BINDER K., NIELABA P. and PEREYRA V., *Z. Phys. B*, **104** (1997) 81.
- [21] GENZER J., FALDI A., OSLANEC R. and COMPOSTO R. J., *Macromolecules*, **29** (1996) 5438.
- [22] SCHWARZ S. A., WILKENS B. J., PUDENSI M. A. A., RAFAILOVICH M. H., SOKOLOV J., ZHAO X., ZHAO W., ZHENG X., RUSSELL T. P. and JONES R. A. J., *Mol. Phys.*, **76** (1992) 937.
- [23] According to ISO 31-8, the term “molecular weight” (M_w) has been replaced with “relative molecular mass” ($M_{r,w}$). The conventional notation, rather than the ISO notation, has been employed for this article.
- [24] GRÜLL H., HAYASHI M., JINNAI H., HASHIMOTO T. and HAN C. C., to be published.
- [25] BERK N. F. and MAJKRZAK C. F., *Phys. Rev. B*, **51** (1995) 11296.
- [26] MAJKRZAK C. F. and BERK N. F., *Physica B*, **268** (1999) 168.
- [27] SCHREYER A., MAJKRZAK C. F., BERK N. F., GRÜLL H. and HAN C. C., *J. Chem. Phys. Solids*, **60** (1999) 1045.
- [28] MAJKRZAK C. F. and BERK N. F., *Phys. Rev. B*, **58** (1998) 15416.
- [29] MAJKRZAK C. F., BERK N. F., DURA J. A., SATIJA S. K., KARIM A., PEDULLA J. and DESLATTES R. D., *Physica B*, **248** (1998) 338.
- [30] MAJKRZAK C. F., BERK N. F., DURA J., SATIJA S. K., KARIM A., PEDULLA J. and DESLATTES R. D., *Physica B*, **241** (1997) 1101.
- [31] MAJKRZAK C. F. and BERK N. F., *Physica B*, **221** (1996) 520.
- [32] MAJKRZAK C. F. and BERK N. F., *Phys. Rev. B*, **52** (1995) 10827.